On the sampling requirements for measuring moments of eddy variability

by G. R. Flierl[1,2] and J. C. McWilliams[1]

ABSTRACT

The expected errors in first and second moments (means, variances, and covariances) calculated from data records of finite length are analyzed, using formulae based on the spectra. The physical processes from which the data are taken are assumed to be stationary and quasi-normal. Asymptotic approximations to these errors (in inverse powers of the record length) are also discussed and compared with the exact expressions. The results are applied to time series measurements of low frequency current variability in the North Atlantic. The magnitudes of the estimated errors, especially in second moments, suggest that the present data sets can be used for qualitative descriptions; however, obtaining precise estimates (10% accuracy) may require prohibitively lengthy experiments.

1. Introduction

This paper addresses the following question: what is the accuracy with which means, variances, and covariances can be calculated from time (or space) series of finite length, and what characteristics of the series are important in determining this accuracy? For any physical system which is random or turbulent (i.e., having important restrictions upon its predictability), the statistical data—the means of various quantities, the intensities of the fluctuations (the variances) and the covariances (such as Reynolds' stresses or eddy heat fluxes)—comprise perhaps the most useful description of its behavior. One oceanic example of such a description comes from measurements of mesoscale eddies and the North Atlantic mean circulation (Schmitz, 1976a and 1976b). Another example is the interaction of internal waves and lower frequency currents (Müller, 1974; Frankignoul, 1976). The mathematical problem of the accuracy of a time average from a finite record as an estimate for the expected value (for a stationary process) is standard and can be found in reference texts such as Bendat and Piersol (1966). One can also find simplified "rule of thumb" estimates of the errors derived by assuming the length of the record (T) is large. Here we offer the following contributions: first, we write the formulae for the expected errors in estimating the mean, variance, and covariance in terms of

1. National Center for Atmospheric Research, Boulder, Colorado, 80303, U.S.A.
2. Permanent affiliation: Dept. of Meteorology, M.I.T., Cambridge, Massachusetts, 02139, U.S.A.

the spectra of the fields, rather than the lagged covariance; second, we write the asymptotic form of the errors (as $T \to \infty$) to 0 (T^{-2}); third, we discuss how these errors depend on the shape and character of the spectrum; fourth, we discuss the accuracy of the asymptotic forms for particular spectral forms; and finally, we use typical oceanic spectra to illustrate application of the formulae and also to indicate the order of the errors in averages from the present data sets.

We have chosen to write our formulae using the spectrum $E(\omega)$ (or the cross-spectrum $E_{ij}(\omega)$), rather than the lagged covariance function $C_{ij}(\omega)$, since the experimentalist generally prefers to discuss the fluctuations in spectral space.[3] Because the raw spectral estimates of the energy in distinct frequency bands are statistically independent, one can average, smooth, or fit models in spectral space to obtain a more plausible estimate of the spectrum. In fact, a covariance function is best smoothed by Fourier transforming to find the spectrum, smoothing in spectral space (thereby avoiding unrealizeable covariance estimates which have negative energy bands), and then transforming back. Furthermore, the uncertainties in a raw spectral estimate are distributed as χ^2 (Jenkins and Watts, 1968), according to the usual theory, whereas covariance uncertainties can only be expressed as a complicated convolution integral. For these reasons we have used $E_{ij}(\omega)$ as the basic description of the random fluctuations, rather than $C_{ij}(\omega)$.

It is characteristic of oceanic spectra (c.f. Figs. 6-8) that they are red (rapidly decreasing) at least above a certain frequency. This feature assures that the high frequency spectral details are not the primary contributors to either the calculated lower moments of variability or to the estimates of their errors (see § 3). In particular, unbiased noise (from frequencies above the Nyquist or from instrumental error) contributes negligibly to the error estimates (see § 4). Similarly the formidable problems of estimation based on unequally spaced data sets or data with gaps can be disregarded if both the spectral peak scales and the extent of the measurements greatly exceed the longest sampling gaps. Thus, in the following, we discuss formulae describing the nature of low frequency and spectral peak contributions to errors in moments calculated from continuous records.

Another simplification will be the assumption that the measurements are from stationary and quasi-normal processes. We assert this not because we believe the ocean truly behaves in this manner, but because the documentation of mesoscale oceanic second moments will be complete long before we discover how poor these assumptions are. For similar reasons, we have restricted ourselves to first and second moments, although our methods are surely extendible to higher moments, because

3. Of course, the formulae can be converted between the spectral and covariance forms by using the relationship

$$E_{ij}(\omega) = \frac{1}{2\pi} \int_{-\infty}^{\infty} d\tau \, C_{ij}(\tau) \, e^{i\omega\tau} \, .$$

present and foreseeable oceanographic observations are not concerned with the higher moments.

2. Expected first and second moment errors for stationary, quasi-normal processes

In this section, we shall write formulae for the expected error of an estimate for the mean or covariance. Some of these formulae are written in standard texts such as Bendat and Piersol (1966) in terms of covariance. Since we are interested in discussing the functional dependence of the errors upon the spectrum, we must either Fourier transform the standard results or rederive them using the Fourier transformed data (see the Appendix for an example).

We denote our data by $\phi_i(t)$ for $t\epsilon\ [-T/2,\ T/2]$. We assume that Fourier transforms of the ϕ_i exist, so that

$$\phi_i(t) = \int_{-\infty}^{\infty} d\omega\, e^{-i\omega t}\, \Phi_i(\omega) + \langle \phi_i \rangle \ , \tag{2.1}$$

where the notation $\langle \bullet \rangle$ represents an ensemble average and Φ is the transform variable. Under the assumption that the process is stationary, we define the cross-spectrum by

$$\langle \Phi_i(\omega)\, \Phi_j(\omega') \rangle = E_{ij}(\omega)\, \delta(\omega + \omega') \tag{2.2}$$

where $E_{ij}(\omega)$ is the cross-spectral density. The *record mean* of ϕ will be denoted by $\bar{\phi}$ and is defined for continuously sampled data by

$$\bar{\phi} = \frac{1}{T}\int_{-T/2}^{T/2} \phi(t)\, dt \ , \tag{2.3}$$

and analogously for discretely sampled data.

a. Error formulae. The expected error variance in an estimate of the true mean of ϕ by the record mean (2.3) is defined as

$$\epsilon_1 = \langle (\bar{\phi} - \langle \phi \rangle)^2 \rangle \ . \tag{2.4}$$

The Appendix shows that this is related to the autospectrum $E(\omega)$ by

$$\epsilon_1 = \int_{-\infty}^{\infty} d\omega\, E(\omega)\, S^2(\omega T/2) \ . \tag{2.5}$$

$S(x)$ is defined as $\overline{\exp(-i2xt/T)}$ and, for the definition of the average (2.3), is just the "sinc" function $(\sin x)/x$ commonly used in spectral analysis.[4]

4. A different definition of the mean (e.g., using discrete samples) will only affect the formulae in this paper by changing the function $S(x)$ from sinc (x) to $\exp(-i2xt/T)$. For discrete samples at spacing $\Delta t = T/(N-1)$

$$S(x) = \frac{1}{N}\,\frac{\sin[x\,(1 + \Delta t/T)]}{\sin[x\,\Delta t/T]} \ .$$

The expected error in the covariance is defined as

$$\epsilon_2 = \langle \{\overline{(\phi_i - \bar{\phi}_i)(\phi_j - \bar{\phi}_j)} - \langle (\phi_i - \langle \phi_i \rangle)(\phi_j - \langle \phi_j \rangle)\rangle\}^2 \rangle$$
$$= \langle \{\overline{\phi_i' \phi_j'} - \overline{\phi_i'}\,\overline{\phi_j'} - \langle \phi_i' \phi_j' \rangle\}^2 \rangle \ , \tag{2.6}$$

where the ϕ' are the true fluctuations $\phi - \langle \phi \rangle$. If we make the quasi-normal assumption that

$$\langle \phi_i' \phi_j' \phi_k' \phi_l' \rangle = \langle \phi_i' \phi_j' \rangle \langle \phi_k' \phi_l' \rangle$$
$$+ \langle \phi_i' \phi_k' \rangle \langle \phi_j' \phi_l' \rangle + \langle \phi_i' \phi_l' \rangle \langle \phi_j' \phi_k' \rangle \ , \tag{2.7}$$

then we can rewrite (2.6) in terms of the spectrum as

$$\epsilon_2 = \int_{-\infty}^{\infty} d\omega \int_{-\infty}^{\infty} d\omega' \, E_{ii}(\omega) \, E_{jj}(\omega') K_A(\omega,\omega') + E_{ij}(\omega) \, E_{ij}(\omega') \, K_B(\omega,\omega') \tag{2.8}$$

where

$$K_A(\omega,\omega') = S^2([\omega - \omega'] \, T/2) + S^2(\omega \, T/2) \, S^2(\omega' \, T/2)$$
$$- 2 \, S([\omega - \omega'] \, T/2) \, S(\omega \, T/2) \, S(\omega' \, T/2)$$
$$K_B(\omega,\omega') = K_A(\omega,\omega') + S^2(\omega \, T/2) \, S^2(\omega' \, T/2) \ . \tag{2.9}$$

Making the familiar partition of the cross-spectrum into the real co-spectrum and quadrature spectrum,

$$E_{ij}(\omega) = P_{ij}(\omega) - \sqrt{-1} \, Q_{ij}(\omega) \ (i \neq j) \ , \tag{2.10}$$

and using the symmetries of E_{ij} and K_B yield

$$\epsilon_2 = \int_{-\infty}^{\infty} d\omega \int_{-\infty}^{\infty} d\omega' \, \{E_{ij}(\omega) \, E_{jj}(\omega') \, K_A(\omega,\omega') +$$
$$[P_{ij}(\omega) \, P_{ij}(\omega') - Q_{ij}(\omega) \, Q_{ij}(\omega')] \, K_B(\omega,\omega')\} \ . \tag{2.11}$$

For the simpler case of estimating the variance or autocovariance (i.e., $i=j$), (2.8) becomes

$$\epsilon_2 = \int_{-\infty}^{\infty} d\omega \int_{-\infty}^{\infty} d\omega' \, E(\omega) \, E(\omega') \, [K_A(\omega,\omega') + K_B(\omega,\omega')] \ . \tag{2.12}$$

We can also compute the relative errors for estimated covariances and variances by dividing (2.11) by $\left\{\int_{-\infty}^{\infty} P_{ij}(\omega) \, d\omega\right\}^2$ and (2.12) by $\left\{\int_{-\infty}^{\infty} E(\omega) \, d\omega\right\}^2$ respectively. (2.5) and (2.11), (2.12) will be our basic equations.

b. Asymptotic approximations. In section *a*, formulae for the expected errors in means, variances, and general second moments were presented. However these are rather complicated and, even for simple spectral shapes, require numerical integration for any practical application. Next we shall derive simpler asymptotic approximations to the errors ϵ_1 and ϵ_2 for large values of the record length T. The requirement for the asymptotic formulae to be useful—that T be large compared to the energetic scales in the spectrum—will be analyzed in more detail in § 3.

The derivation of the asymptotic formulae depends on two theorems given in the Appendix. Based on these results we can write

$$\epsilon_1 \sim \frac{2\pi}{T} E(0) + \frac{2}{T^2}\int_{-\infty}^{\infty} d\omega \, \frac{E(\omega) - E(0)}{\omega^2} + o\left(\frac{1}{T^N}\right) \tag{2.13}$$

(for any finite value of N) and

$$\epsilon_2 \sim \frac{2\pi}{T}\int_{-\infty}^{\infty} d\omega \, [E_{ii}(\omega) E_{jj}(\omega) + P_{ij}^2(\omega) - Q_{ij}^2(\omega)]$$
$$+ \frac{2}{T^2}\left\{\int_{-\infty}^{\infty}\frac{d\tau}{\tau^2}\int_{-\infty}^{\infty} d\omega \left[E_{ii}\left(\omega + \frac{\tau}{2}\right) E_{jj}\left(\omega - \frac{\tau}{2}\right) - E_{ii}(\omega) E_{jj}(\omega)\right.\right.$$
$$+ P_{ij}\left(\omega + \frac{\tau}{2}\right) P_{ij}\left(\omega - \frac{\tau}{2}\right) - P_{ij}^2(\omega) - Q_{ij}\left(\omega + \frac{\tau}{2}\right) Q_{ij}\left(\omega - \frac{\tau}{2}\right)$$
$$\left.\left. + Q_{ij}^2(\omega)\right] - 2\pi^2 E_{ii}(0) E_{jj}(0)\right\} + 0\left(\frac{1}{T^3}\right). \tag{2.14}$$

For the variance error (2.12), the asymptotic approximation is

$$\epsilon_2 \sim \frac{4\pi}{T}\int_{-\infty}^{\infty} d\omega \, E^2(\omega)$$
$$+ \frac{4}{T^2}\left\{\int_{-\infty}^{\infty}\frac{d\tau}{\tau^2}\int_{-\infty}^{\infty} d\omega \left[E\left(\omega + \frac{\tau}{2}\right) E\left(\omega - \frac{\tau}{2}\right) - E^2(\omega)\right]\right.$$
$$\left. - \pi^2 E(0)\right\} + 0(1/T^3). \tag{2.15}$$

We can see that the asymptotic formulae are simple in the sense that the integrals over the spectrum need be done only once, whereas the correct formulae (2.5), (2.11), (2.12) need to be reintegrated each time T is changed.

The order $1/T$ asymptotic approximations are found in standard texts in terms of the covariances; for example, the first term in (2.13) (which we define to be $\epsilon_1^{(1)}$) is just

$$\epsilon_1^{(1)} = \frac{2\pi E(0)}{T} = \frac{2}{T}\int_0^{\infty} d\tau \, C(\tau) \equiv 2\frac{\sigma^2 \tau_I}{T}, \tag{2.16}$$

where σ^2 is the variance (i.e., $C(0)$) and τ_I is the integral time scale (Lumley and

Panofsky, 1964). Bendat and Piersoll (1966) also give the first asymptotic term for the second moment error

$$\epsilon_2{}^{(1)} = \frac{4\pi}{T}\int_{-\infty}^{\infty} d\omega\, E^2(\omega)$$

$$= \frac{2}{T}\int_{0}^{\infty} d\tau\, C^2(\tau)\ , \tag{2.17}$$

in the special case of variance estimation.

The order $1/T^2$ contributions to the errors are much less familiar and are rarely included in error estimates; however, we shall show below that their inclusion significantly improves the accuracy of the asymptotic formulae (2.13-15). We should also mention that the simplicity of the asymptotic formulae is somewhat misleading since our attempts to evaluate (2.5), (2.11-12) and (2.13-15) for various test spectra indicate that the integrals in the asymptotic formulae are considerably more sensitive to the numerical techniques used than are the exact formulae.

3. Contributions of various parts of the spectrum to mean and covariance errors

We can illustrate the contributions of various regions of the spectrum by using a test spectrum. Consider a Gaussian spectral component

$$\Delta(\omega) = \frac{\alpha T}{2\pi\sqrt{\pi}} \exp\left[-(\alpha\omega T/2\pi)^2\right] \tag{3.1}$$

which has unit total energy (i.e., unit frequency integral) and a bandwidth $0(\alpha^{-1})$ in the frequency variable $x = \omega T/2\pi$. We shall choose an 0(1) bandwidth in x since, in practice, one has no knowledge on any finer bandwidths from a finite record length T; therefore it seems appropriate to discuss test spectra which average over this bandwidth in frequency. We have used $\alpha = 2.25$ for the following plots and discussions, but the results are not especially sensitive to this choice. x is also the natural variable for discussing the $S^2(\omega T/2)$ weighting function in (2.5) because $S^2(\omega T/2)$ has zeros at $x = 1, 2, 3 \ldots$

A sequence of test spectra $D_n{}^{\pm}(\omega)$ will be defined by

$$D_n{}^{\pm}(\omega) = \frac{1}{2}\left[\Delta\left(\omega - \frac{2\pi}{T}\, n\right) \pm \Delta\left(\omega + \frac{2\pi}{T}\, n\right)\right] \tag{3.2}$$

for $n = 0, 1, 2 \ldots$ This test spectrum can be considered a component in the following representation of an actual spectrum:

$$E(\omega) = \sum_{n=0}^{\infty} e_n\, D_n{}^{+}(\omega)\ . \tag{3.3}$$

The amplitudes e_n in (3.3) would be defined by

$$e_n \approx \int_{2\pi/T\,(n-\frac{1}{2})}^{2\pi/T\,(n+\frac{1}{2})} d\omega\,[E(\omega) + E(-\omega)]$$
$$\approx \frac{4\pi}{T} E\left(2\pi n/T\right) \tag{3.4}$$

since $E(\omega)$ is an even function.

Thus as our record length T increases, the frequency corresponding to a given n decreases and the amplitudes e_n also tend to decrease. Alternately a given spectral peak in $E(\omega)$ will, as T increases, be associated with higher values of n, be broader in Δ_n and decrease in amplitude e_n.

If we expand $E(\omega)$, $E_{ii}(\omega)$, $E_{jj}(\omega)$ and $P_{ij}(\omega)$ in the $D_n^+(\omega)$ functions as in (3.3) and $Q_{ij}(\omega)$ in the $D_n^-(\omega)$ functions (which are odd functions of frequency), we can write the error in the mean as

$$\epsilon_1 = \sum_n e_n \left[\int_{-\infty}^{\infty} d\omega\, D_n^+(\omega)\, S^2\left(\omega T/2\right)\right], \tag{3.5}$$

the error in the variance as

$$\epsilon_2 = \sum_n \sum_m e_n\, e_m \left[\int_{-\infty}^{\infty} d\omega \int_{-\infty}^{\infty} d\omega' \{K_A(\omega,\omega') + K_B(\omega,\omega')\} D_n^+(\omega)\, D_m^+(\omega')\right], \tag{3.6}$$

and the error in the covariance as

$$\epsilon_2 = \sum_n \sum_m e_n^{ii}\, e_m^{jj} \left[\int_{-\infty}^{\infty} d\omega \int_{-\infty}^{\infty} d\omega'\, K_A(\omega,\omega')\, D_n^+(\omega)\, D_m^+(\omega')\right]$$
$$+ \sum_n \sum_m p_n^{ij}\, p_m^{ij} \left[\int_{-\infty}^{\infty} d\omega \int_{-\infty}^{\infty} d\omega'\, K_B(\omega,\omega')\, D_n^+(\omega)\, D_m^+(\omega')\right]$$
$$+ \sum_n \sum_m q_n^{ij}\, q_m^{ij} \left[\int_{-\infty}^{\infty} d\omega \int_{-\infty}^{\infty} d\omega'\, K_B(\omega,\omega')\, D_n^-(\omega)\, D_m^-(\omega')\right]. \tag{3.7}$$

The terms in the square brackets in equations (3.5-7) have been plotted or contoured in Figures 1 through 5. That is, we have plotted

$$\epsilon_1(n) = \int_{-\infty}^{\infty} d\omega\, D_n^+(\omega)\, S^2\left(\omega T/2\right) \tag{3.8}$$

$$\epsilon_2(n,m) = \int_{-\infty}^{\infty} d\omega \int_{-\infty}^{\infty} d\omega' \left[K_A(\omega,\omega') + K_B(\omega,\omega')\right] D_n^+(\omega)\, D_m^+(\omega') \tag{3.9}$$

and similar cospectral and quadrature spectral terms.

Note that each of these is independent of T; all of the T dependence enters in the relationships between n and ω and between e_n and the spectral energy. We have

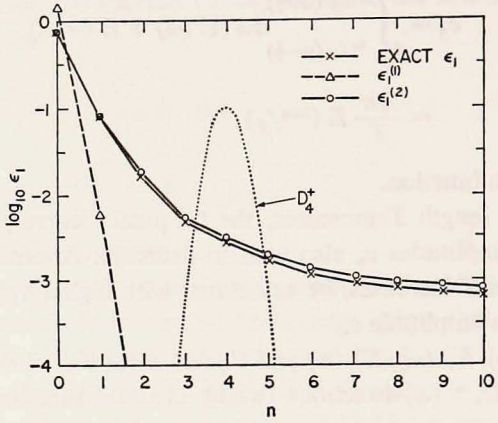

Figure 1. The contributions to first moment error for the Gaussian spectra (3.2). Also shown is D_4^+ plotted for frequency $\omega = n\ 2\pi/T$ (where n is regarded as a continuous variable). Three formulae are shown: the exact ϵ_1 from (3.8), the first asymptotic approximation (3.10), and the combined approximation (3.11).

also plotted the equivalent bracketed terms which would occur in the asymptotic formulae (2.13-15) upon substitution of expansions such as (3.3); these terms are defined by

$$\epsilon_1^{(1)}(n) = {}^{2\pi}/_{T}\, D_n^+(0) \tag{3.10}$$

$$\epsilon_1^{(2)}(n) = {}^{2\pi}/_{T}\, D_n^+(0) + {}^{2}/_{T^2} \int_{-\infty}^{\infty} \frac{D_n^+(\omega) - D_n^+(0)}{\omega^2}\, d\omega \tag{3.11}$$

$$\epsilon_2^{(1)}(n,m) = {}^{4\pi}/_{T} \int_{-\infty}^{\infty} d\omega\, D_n^+(\omega)\, D_m^+(\omega) \tag{3.12}$$

$$\epsilon_2^{(2)}(n,m) = \epsilon_2^{(1)}(n,m) +$$

$$\frac{4}{T^2}\left\{ \int_{-\infty}^{\infty} d\tau/\tau^2 \int_{-\infty}^{\infty} d\omega\, [D_n^+(\omega + {}^{\tau}/_{2})\, D_m^+(\omega - {}^{\tau}/_{2}) - D_n^+(\omega)\, D_m^+(\omega)] - \pi^2 D_n^+(0)\, D_m^+(0) \right\} \tag{3.13}$$

etc.

a. Error in the mean. Figure 1 shows the contribution to the error in the mean from various parts of the spectrum. The energy in the unresolved band (n=0) contributes with the greatest weight to the error; it is adequately represented by both the one and two-term asymptotic approximations (though the one-term form somewhat overestimates ϵ_1 (0)). The energy in the marginally resolved band (n=1) is weighted by a factor an order of magnitude smaller than that of the unresolved band, but now the single term estimate $\epsilon_1^{(1)}$ is much too small. These features are also characteristic of the better resolved bands ($n > 1$), whose contribution to the

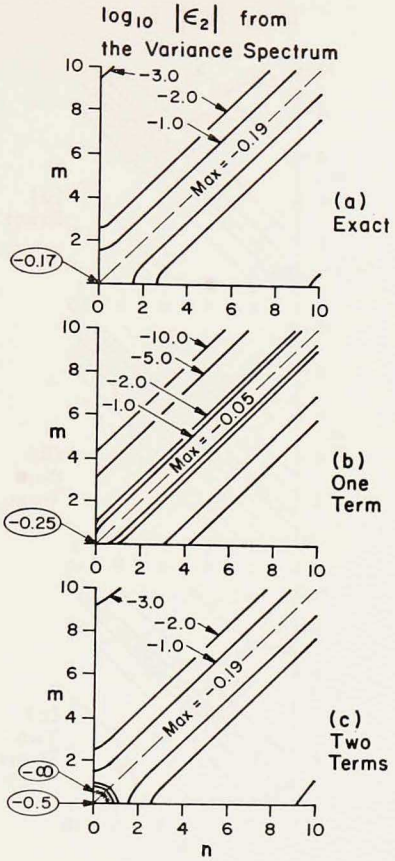

Figure 2. The contributions to variance error for Gaussian spectra (3.2). The three panels are (a) the exact ϵ_2 from (3.9), (b) $\epsilon_2^{(1)}$ from (3.12), and (c) the two-term approximation (3.13).

total ϵ_1, per unit energy in the band, decreases as n^{-2}. These results lead to a few simple rules: if the actual spectrum is red, then the major contribution to ϵ_1 comes from the unresolved band ($\omega < {}^{2\pi}/_{T}$) and the simple single-term formula (2.16) will adequately, even conservatively, estimate the error. However, if the spectrum is strongly peaked at frequencies greater than ${}^{2\pi}/_{T}$, then either (2.13) or the exact formula (2.5) must be used.

b. Error in the variance. In Figure 2 are shown ϵ_2 (n,m) from (3.9), $\epsilon_2^{(1)}$ (n,m) from (3.12) and $\epsilon_2^{(2)}$ (n,m) from (3.13). The contributions are most strongly weighted along the diagonal $m = n$, where the weighting is fairly uniform. The one term formula $\epsilon_2^{(1)}$ (n,m) generally overestimates the exact ϵ_2 by about 50% over most of the diagonal region and by more than 100% in the doubly unresolved band ($n = m = 0$). Away from the diagonal $\epsilon_2^{(1)}$ is a gross underestimate of ϵ_2. The two-

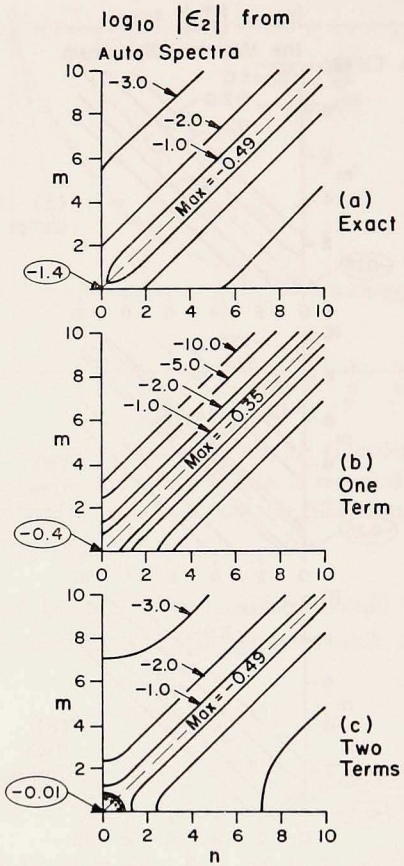

Figure 3. The contributions to covariance error for the bracketed autospectral quantity in (3.7) with Gaussian test spectrum (3.2). The three panels are (a) the exact ϵ_2, (b) $\epsilon_2^{(1)}$, and (c) $\epsilon_2^{(2)}$ —which have been defined similarly to (3.9), (3.12), (3.13). The sign of ϵ_2 is positive everywhere except near $m = n = 0$ in (c).

term expansion is a satisfactory representation of ϵ_2 everywhere except in the unresolved bands, where it yields a slight overestimate (less than 10%). At the origin, though, $\epsilon_2^{(2)}$ is a nonsensical negative number. The asympototic forms for variance are unsatisfactory for the doubly unresolved band, and may be successfully used only when the amount of energy there is small. If there is much energy in any of the other unresolved bands (i.e., if the products $e_0 e_m$ are not relatively small in (3.16)), then the two-term approximation will be an overestimate. Nowhere is the first term approximation very accurate.

c. Error in the covariance. The contribution to covariance errors from the autospectral terms is shown in Figure 3. The heaviest weighting is along the diagonal with a moderate decrease in the unresolved band; thus our ignorance of this band

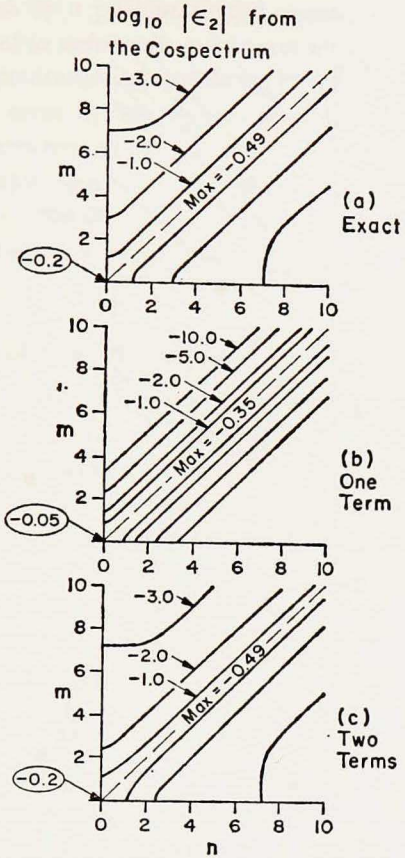

Figure 4. The counterpart to Figure 8 for cospectra.

is not as serious as it is for variance. The "equal frequency" dominance implies that if one process is band limited, then we need examine the other process only in this band. The one term approximation $\epsilon_2{}^{(1)}$ (n,m) is qualitatively similar to ϵ_2 (i.e., within 50%) for the diagonal band $m = n$ (except $m = n = 0$) and the nearest off-diagonal bands. However, it decreases much too rapidly for more widely separated bands. The two term estimate $\epsilon_2{}^{(2)}$ (n,m) is quite accurate except at the origin (where it gives a fallacious negative contribution). Thus, if the actual spectra, E_{ii} (ω) and E_{jj} (ω), are both narrow band and similar in their shapes, then either of the one or two-term approximations will give similar estimates; if there is much energy in the unresolved band for this case, then they will not well represent its contribution. For autospectra of dissimilar shapes, the two-term approximation will be clearly superior, and, unless *both* autospectra are red, it will be reasonably accurate.

The error contributions from the cospectral terms (i.e., terms with P_{ij} (ω)) are shown in Figure 4. Again the diagonal terms dominate and the off-diagonal weight-

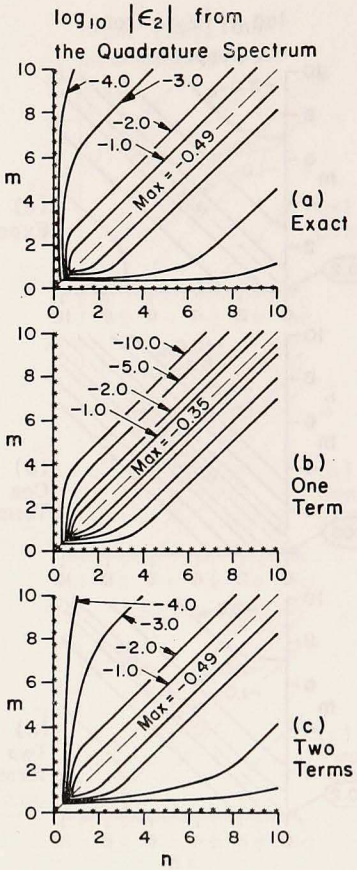

Figure 5. The counterpart to Figure 8 for quadrature spectra. The sign of the contribution is the same as that of $-m \cdot n$.

ings are several orders of magnitude smaller. Now, however, the doubly unresolved band at the origin is the most heavily weighted region; the error is dominated by the "equal frequency" contribution with a slight predominance in the unresolved band. The asymptotic estimates of the contribution are of similar quality as those discussed for variance errors. The two term estimate is everywhere excellent (even at the origin) but the one term estimate is conservative along the diagonal and greatly underestimates the contributions elsewhere.

Finally we have plotted the contribution of various parts of the quadrature spectrum in Figure 5. The weighting is negative in the $n,m > 0$ quadrant, is maximum on the diagonal and decreases to zero for either n or $m = 0$. Since the coefficients q_n^{ij} may be of either sign, the contribution of the quadrature term could be positive or negative. However, since the dominant contribution is from the diagonal region,

which will be multiplied by a positive $[q_n^{ij}]^2$, we expect the quadrature spectrum terms will in general tend to *reduce* the total error in (2.11). The single term asymptotic estimate of the quadrature contribution is again an overestimate along the diagonal (reducing the error by too much) and an underestimate elsewhere. The two term formula is everywhere accurate.

In summary, the major contributions to the covariance terms come from the diagonal $m = n$ parts of the integrals. The two term asymptotic formula will be fairly accurate unless there is a sizeable amount of energy in the unresolved bands of both autospectra.

4. Oceanic applications of a model spectrum

In practice there are often few pieces of information which can be determined from a measured spectrum with any accuracy; for example, turbulent subrange spectra are often summarized by only an overall amplitude and a power law exponent. In this spirit we introduce a three parameter auto-spectrum for purposes of demonstrating certain simple functional dependences in the errors ϵ_1 and ϵ_2 and for applications to observations of mesoscale eddies.

The model spectrum is chosen to be even in ω, analytic as $\omega \to 0$, rapidly decaying to zero as $\omega \to \infty$, and capable of representing a spectral peak at intermediate frequencies; explicitly, the form is

$$E_M(\omega) = E_0 [1 + \eta (\omega/\omega_0)^2] \exp [-(\omega/\omega_0)^2] \ . \tag{4.1}$$

Various characteristics of E_M are listed in Table 1, including the consequent expected mean and variance errors and their asymptotic expansions through two powers of $1/T$; the formulae for these quantities are listed in § 2. Notice that, in addition to terms proportional to $1/T$ or $1/T^2$ in ϵ_1, the remaining terms behave as $\exp(-T^2)/T$, etc.—they decay faster than any power of $1/T$ as $T \to \infty$ (see (2.13)). Listed are general results plus their limiting forms in the alternative limits of $\eta \to 0$ (a red spectrum) and $\eta >> 1$ (a highly peaked one).

a. Asymptotic validity. One use of the three parameter model is as a tool in examining details of the dependence of error upon record length. If we divide the first and second moment error formulae in Table 1 by $E_0\omega_0$ and $(E_0\omega_0)^2$, respectively, then these normalized errors are functions only of η and $T^* = \omega_0 T/2$, the record length multiplied by half the characteristic decay rate in (4.1). Shown in Figure 6, therefore are expected mean and variance errors $v.$ T^* for different values of η.

For errors in the mean, the first approximation $\epsilon_1^{(1)}$ is an underestimate of the actual ϵ_1 for $\eta > 2$ and an overestimate for $\eta < 2$. Because of this behavior, the $\epsilon_1^{(1)}$ approximation is an accurate one for moderate T^* only within an intermediate range of η values (e.g. only the $\eta = 1$, 1.5, and 2 plots exhibit 10% accuracy by $T^* = 4$). The two-term approximation, however, is generally quite accurate for all

Table 1. A Three Parameter Auto-Spectrum.

Feature	General form
Covariance function $C(\tau)$	$E_0\omega_0 \sqrt{\pi}\left(1+\frac{\eta}{2}\right) e^{-\tau^2\omega_0^2/4} \cdot \left(1-\frac{\eta}{1+\frac{\eta}{2}}\frac{\tau^2\omega_0^2}{4}\right)$
Variance σ^2	$E_0\omega_0 \sqrt{\pi}\left(1+\frac{\eta}{2}\right)$
Integral scale τ_I	$\frac{\sqrt{\pi}}{\omega_0}\frac{2}{2+\eta}$
Covariance function zero crossing τ_c	$\frac{2}{\omega_0}\sqrt{\frac{2+\eta}{2\eta}}$
Time scale of spectral maximum τ_M	$\begin{cases}\infty \text{ for } \eta \leqslant 1 \\ \frac{1}{\omega_0}\sqrt{\frac{\eta}{\eta-1}} \text{ for } \eta > 1\end{cases}$
Spectral maximum $E(1/\tau_M)$	$\begin{cases}E_0 & \eta \leqslant 1 \\ E_0\eta e^{-[1-(1/\eta)]} & \eta > 1\end{cases}$
Time scale of $\omega E(\omega)$ maximum τ'_M	$\frac{1}{\omega_0}\sqrt{\frac{4\eta}{3\eta-2+\sqrt{9\eta^2+4+2\eta}}}$
Spectral maximum $\frac{1}{\tau'_M}E(1/\tau'_M)$	$\frac{E_0}{\tau'_M}\left(1+\frac{\eta}{(\tau'_M\omega_0)^2}\right) e^{-(\tau'_M\omega_0)^2}$
Error in the mean ϵ_1	$E_0\frac{2\pi}{T}\operatorname{erf}\frac{\omega_0 T}{2} + \frac{E_0}{\omega_0}\left(\frac{\eta}{2}-1\right)\sqrt{\pi}\left(\frac{2\pi}{T}\right)^2\left(1-e^{-(\omega_0 T/2)^2}\right)$
Asymptotic error in the mean $\epsilon_2^{(2)}$	$E_0\frac{2\pi}{T} + \frac{E_0}{\omega_0}\left(\frac{\eta}{2}-1\right)\sqrt{\pi}\left(\frac{2\pi}{T}\right)^2$
Error in the variance	$\iint d\omega\, d\omega'\, E(\omega)E(\omega')(K_A+K_B)$
Asymptotic error in variance $\epsilon_2^{(2)}$	$\frac{(2\pi)^{3/2}}{T}E_0^2\omega_0\left(1+\frac{\eta}{2}+\frac{3}{16}\eta^2\right) - \frac{4\pi}{T^2}E_0^2\left(1+\pi+\frac{\eta^2}{4}\right)$

$\eta = 0$	$\eta \to \infty$
$E_0\omega_0 \sqrt{\pi}\, e^{-\tau^2\omega_0^2/4}$	$E_0\omega_0 \sqrt{\pi}\,\frac{\eta}{2}\left[1-\frac{\tau^2\omega_0^2}{2}\right] e^{-\tau^2\omega_0^2/4}$
$E_0\omega_0 \sqrt{\pi}$	$E_0\omega_0 \sqrt{\pi}\,\frac{\eta}{2}$.
$\frac{\sqrt{\pi}}{\omega_0}$	$\frac{2\sqrt{\pi}}{\omega_0\eta}$
∞	$\frac{\sqrt{2}}{\omega_0}$
∞	$\frac{1}{\omega_0}$
E_0	$E_0\eta e^{-1}$
$\frac{\sqrt{2}}{\omega_0}$	$\frac{1}{\omega_0}\sqrt{\frac{2}{3}}$
$\frac{E_0\omega_0}{\sqrt{2}}\, e^{-1/2}$	$E_0\omega_0\left(\frac{3}{2}\right)^{3/2}\eta e^{-3/2}$
$E_0\frac{2\pi}{T}\,\mathrm{erf}\,\frac{\omega_0 T}{2}$	$\frac{\eta}{2}\,\frac{E_0}{\omega_0}\sqrt{\pi}\left(\frac{2\pi}{T}\right)^2\left(1-e^{-(\omega_0 T/2)^2}\right)$
$-\frac{E}{\omega_0}\sqrt{\pi}\left(\frac{2\pi}{T}\right)^2\left(1-e^{-(\omega_0 T/2)^2}\right)$	
$E_0\frac{2\pi}{T} - \frac{E_0}{\omega_0}\sqrt{\pi}\left(\frac{2\pi}{T}\right)^2$	$\frac{\eta E_0}{2\omega_0}\sqrt{\pi}\left(\frac{2\pi}{T}\right)^2$
$E_0^2\int\int e^{-(\omega/\omega_0)^2-(\omega'/\omega_0)^2}\,(K_A+K_B)\,d\omega d\omega'$	$E_0^2\eta^2\int\int\frac{\omega^2\omega'^2}{\omega_0^4}\, e^{-(\omega/\omega_0)^2-(\omega'/\omega_0)^2}$ $\cdot\,(K_A+K_B)\,d\omega d\omega'$
$\frac{(2\pi)^{3/2}}{T}E_0^2\omega_0 - \frac{4\pi}{T}E_0^2(1+\pi)$	$E_0^2\eta^2\left[\frac{3}{16}\,\frac{(2\pi)^{3/2}\omega_0}{T} - \frac{\pi}{T^2}\right]$

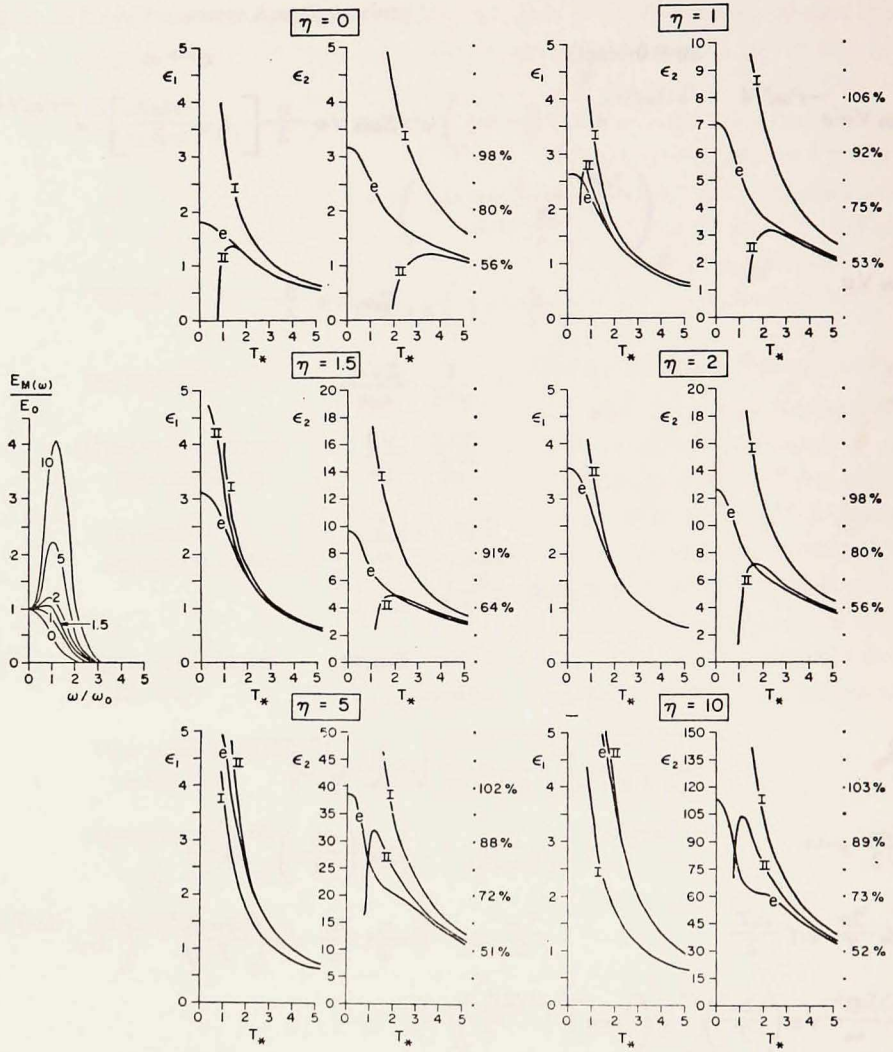

Figure 6. A set of plots for six values of η of expected errors v. T^* from the three parameter spectrum (4.1). In the left half of each panel is $(\epsilon_1/E_0\omega_0)$; the right half is $(\epsilon_2/E_0^2\omega_0^2)$. For each of these, the exact (e), one-term (I), and two-term (II) error forms are plotted. In the variance case a vertical axis is appended which interprets the variance errors as percentage accuracies (i.e., $100 \times \sqrt{\epsilon_2/\sigma^2}$). A small plot of $E_M(\omega)$ is also included for each η value at the side of the figure.

$T^* \gtrsim 1.5$ independent of the η value. Near the T^* origin, $\epsilon_1^{(2)}$ diverges considerably from ϵ_1. Notice from Table 1 that the requirement for the second term to contribute as much as $\epsilon_1^{(1)}$ in the asymptotic estimate is that $\eta > 2\ (\sqrt{\pi}\ T^* + 1)$. If, in addition, this condition should hold while the two-term approximation is an accurate

one ($T^* \gtrsim 1.5$), then we require $\eta \gtrsim 7$; thus, if the spectrum is highly peaked, the two-term approximation is markedly superior to $\epsilon_1^{(1)}$.

For the variance errors the time required for accurate estimates by the asymptotic forms is somewhat larger; generally, the values for the exact and two term approximations are within 10% of each other for $T^* \gtrsim 4$. The first term approximation is always an overestimate of ϵ_2; $\epsilon_2^{(2)}$ diverges to negative values as $T^* \to 0$ and at intermediate values is either an over or underestimate depending upon whether η is greater than or less than about 1.5. The $\epsilon_2^{(1)}$ estimate is generally within 10% of ϵ_2 for T_* values of between 5 and 20, depending upon whether η is large or small. As remarked following (2.12), it is possible to estimate relative errors by normalizing $\sqrt{\epsilon_2}$ by the variance σ^2 (this relative measure has been included in Figure 6 as an additional ordinate). Notice that for all values of η in Figure 6, one still must expect an uncertainty of greater than 50% in estimates of σ^2 even by $T_* = 5$. Contrary to the case of ϵ_1, for ϵ_2 it is the small η cases (red spectra) in which the $0(1/T_*^2)$ corrections are most important for assuring successful asymptotics at modest T^* values.

b. A noise model. We may employ the model (4.1) for $\eta = 0$ and $\omega_0 \equiv \omega_N >> \frac{1}{T}$ to represent an unbiased noise spectrum with time scales very much smaller than the record length. If we define $E_N = \sigma_N^2/\omega_N \sqrt{\pi}$, then σ_N^2 is the finite noise variance and the covariance function

$$C(\tau) = \sigma_N^2 \exp[-(\tau \omega_N/2)^2]$$

has a correlation time $1/\omega_N$ which is very much smaller than T. The noise contribution to the asymptotic mean error is

$$\epsilon_1^{(2)} = \sigma_N^2 \frac{1}{\sqrt{\pi}\,\omega_N T}\left(\pi - \frac{2\sqrt{\pi}}{\omega_N T}\right)$$

which goes to zero for large $\omega_N T$. If we compare the contributions to the error from both the noise and the mesoscale (using $\epsilon_1^{(1)}$), we find that the ratio of the two contributions is $\sigma_N^2 \omega_0 (1 + \eta/2)/\sigma^2 \omega_N$ which is negligible if the noise variance is small compared to the signal variance or if the noise time scale is sufficiently short. Similarly, the $\epsilon_2^{(1)}$ form is proportional to $\sigma_N^4/\omega_N T$. When the preceding noise spectrum is a component of a more complicated spectrum, then all terms contributing to expected errors, which depend upon $\sigma_N^2 \neq 0$, are also proportional to $1/\omega_N T$. This, then, justifies our neglect of noise contributions to moment errors.

c. Deep ocean spectra from the Western North Atlantic. Long time series from the mid-ocean are presently somewhat rare, though much effort is being expended to acquire more. In this section we shall examine three autospectra and estimate from them the expected errors in the calculated means and variances. The following cases were selected: a temperature spectrum in the main thermocline near Bermuda

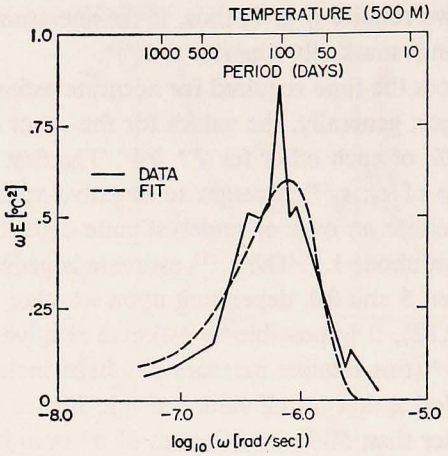

Figure 7. A temperature spectrum from the main thermocline near Bermuda (from Wunsch, 1972) plus the optimal fit (4.3) within the three parameter model (4.1). Only the positive frequency parts of the spectra are plotted; to obtain the total contribution associated with a particular $|\omega|$, the amplitudes here should be doubled.

(Wunsch, 1972), and two kinetic energy spectra from current meter moorings in the center of the MODE region (Schmitz, personal communication)—one at 500 m and the other at 4000 m depth. Respectively, these will be referred to as T_{500}, V_{500}, and V_{4000}. The first of these is a very long record (about 6 years) while the latter two are around 2 years.

We have used two different methods to estimate the moment errors from the data spectra. The first involves interpolating between data values and evaluating the exact error formulae by trapezoidal quadrature. The second method fits the free parameters of the model spectrum (4.1) to the data and calculates errors from the formulae in Table 1. For the fit a least-squares minimization procedure was used with two alternative forms for the minimized error norms between the data and the fit; they were finite series approximations to either

$$\int_{-\infty}^{\infty} d\omega \, (E_{\text{data}} - E_M)^2 \tag{4.2}$$

or

$$\int_{-\infty}^{\infty} d \log_{10} \omega \, [\omega \, E_{\text{data}} - \omega \, E_M]^2 \ . \tag{4.3}$$

These yield fits which best approximate the observations on either an (E *v.* ω) plot or an "energy preserving" (ωE *v.* $\log_{10}\omega$) plot. The results from the latter are compared with the data spectra in Figures 7-9. The optimal parameters from both cases, as well as the expected moment errors, are listed in Table 2. One can note immediately that the parameters selected from (4.2) and (4.3) are not identical: the

Table 2. Error Estimates for Data.

Spectrum	Method	$E(0)$ [$\times 10^6$ °$C^2 s$]	η	ω_0 [d^{-1}]	σ^2 [°C^2]	$\sqrt{\epsilon_1}$ [°C] (T=100d,300d,700d)	$\sqrt{\epsilon_2}$ [°C^2] (T=100d,300d,700d)	$\sqrt{\epsilon_2}/\sigma^2$
T_{500}	(4.2)	1.2	1.0	1/15	2.5	(.9, .5, .3)	(1.5,1.0,.6)	(.6,.4,.2)
	(4.3)	1.3	0	1/11	2.5	(.9, .5, .3)	(1.5,1.0,.7)	(.6,.4,.3)
	quadrature	1.0	—	—	2.8	(.9, .5, .3)	(1.5,1.0,.7)	(.6,.4,.2)
	quadrature	5.0	—	—	3.0	(1. , .7, .6)	(1.5,1.1,.7)	(.5,.4,.2)
		[$\times 10^7$ cm^2 s^{-1}]		[d^{-1}]	[cm^2/sec^2]	[cm/sec]	[cm^2/sec^2]	
V_{500}	(4.2)	10.8	0	1/21	104	(7.5,4.2,2.7)	(70,54,38)	(.7,.5,.4)
	(4.3)	10.6	0	1/24	90	(7.3,4.1,2.5)	(66,48,34)	(.7,.5,.4)
	quadrature	4.	—	—	112	(6.9,3.5,2.1)	(74,58,40)	(.7,.5,.4)
	quadrature	20.	—	—	132	(8.6,6.4,4.4)	(82,62,46)	(.6,.5,.4)
		[$\times 10^6$ cm^2 s^{-1}]		[d^{-1}]	[cm^2/sec^2]	[cm/sec]	[cm^2/sec^2]	
V_{4000}	(4.2)	3.2	4.7	1/12	18.2	(1.7,1. , .6)	(11. ,6.4,4.2)	(.6,.4,.2)
	(4.3)	5.4	1.8	1/11	19.6	(1.8,1.1, .7)	(11.2,6.8,4.4)	(.6,.3,.2)
	quadrature	2.	—	—	19.8	(1.6, .7, .4)	(11.2,6.8,4.6)	(.6,.3,.2)
	quadrature	10.	—	—	20.8	(2. ,1.4,1.)	(11.4,7.2,4.8)	(.5,.3,.2)

weighting given to different parts of the spectra are quite different in the two cases. The largest discrepancy occurs in V_{4000} where there is some uncertainty about whether the spectral peak should be fit by a large E_0 and intermediate η value or

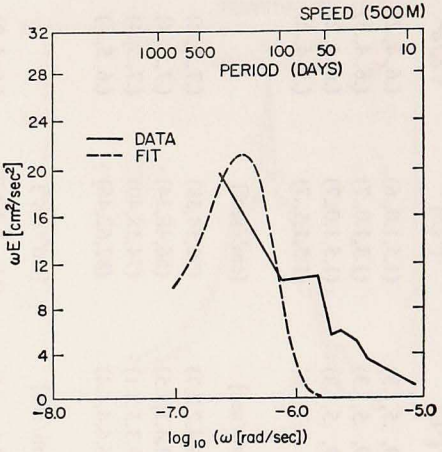

Figure 8. A kinetic energy spectrum from 500 m depth near 28°N, 70°W (from Schmitz, personal communication) plus the optimal fit.

vice-versa. The consequent expected errors, however, are not sensitive to this parameter uncertainty.

Another aspect of imperfection in the fit is shown in Figure 8; the shape of the V_{500} spectrum is not particularly similar to the model (4.1). The peak in $\omega E(\omega)$ is not resolved in the data and the high frequency decay is much weaker than exponential. Nevertheless, the predicted errors from the fit match reasonably well those from direct quadrature.

Some insight into the behavior of the errors as a function of T and of the asymptotic formulae can be gained by referring to Figure 6 for the relevant η values (recalling that $T^* = 1$ corresponds to $T = 2/\omega_0$). Here we shall note only that the simple one term asymptotic formula for the error in the mean $\epsilon_1^{(1)}$ is accurate for the 300 day estimates for T_{500} and V_{4000} and for all 700 day estimates, whereas the two term formula $\epsilon_1^{(2)}$ is accurate for the whole table. For the variance errors, $\epsilon_2^{(1)}$ is only accurate for the 700 day estimates of T_{500} and V_{4000}; $\epsilon_2^{(2)}$ is accurate for all estimates at 300 and 700 days. Thus we can see that the simple standard asymptotic formulae of order $1/T$ may be inaccurate for the time intervals commonly used for moored instrument deployment.

For the alternate approach of fitting an interpolating function to E_{data} we used cubic splines with $\partial\epsilon/\partial\omega = 0$ at both $\omega = 0$ and the highest frequency. $E(0)$ is an unknown constant which was chosen by simple extrapolation; however, we also used the E_0 values from the three parameter model fits as a guide for this choice. The estimates of the errors from this method are also shown in Table 2 along with the errors from a more conservative choice of $E(0)$ (a factor of 5 larger than the first choice). ϵ_1 is the only error which is a sensitive function of $E(0)$. It is encourag-

ing to see that both the model fitting and the direct quadrature give quite similar results. This confirms *a posteriori* that our methods for estimating ϵ_1 and ϵ_2 are not particularly sensitive to the parts of the spectrum which may not be adequately modeled by (4.1) or to the necessarily unknown $E(0)$ value.

Finally we shall discuss the implications of the results in Table 2 for the accuracy of present mesoscale observations. The mean temperature at 500 m in the Bermuda area is on the order of 17°C; thus the relative errors in this quantity are quite small even for short time periods. However, large-scale, mid-ocean horizontal temperature gradients at 500 m may be only 5°/1000 km, and measurements to 10% accuracy of differences of mean temperature of the order of 5° would require $\sqrt{\epsilon_1} \approx .1$ $(1/\sqrt{2})\ 5° = .35°$ or measurement times $\gtrsim$ 700 days. Similarly, even the 700 day estimates of the variance in T' are only of 20-30% accuracy, and, for a more typical mooring lifetime of 300 days, the estimates are quite inaccurate.

The mean velocities at 500 and 4000 m have been estimated as 1.3 ± 1.2 cm/sec and .3 ± .4 cm/sec, respectively (Schmitz, personal communication). The uncertainties quoted are "stability" estimates, derived by finding the changes in the average of the series when the most energetic or least energetic records are discarded. An average of our estimates for the errors in these means (from Table 2) gives ± 3 and ± 6 after 700 days; thus neither mean is distinguishable from zero. 300 day measurements give only crude estimates of the variances and virtually no information about the mean. (The error estimates from our formulae tend to be somewhat larger than the stability estimates of Schmitz, since his estimates in some sense consider only the error contribution from the resolved part of the spectrum, while ours include, albeit approximately, the contribution from the unresolved part also). Schmitz (1976a) gives a 700 day estimate of eddy velocity variance at 4000 m of 17.3 ± 3.0 cm²/sec². He also reports that the estimates settled down to within his tolerance after 250-300 days. This may seem surprising since Table 2 indicates the errors in a 300 day variance should be ± 11 cm²/sec²; however, the probability that the averages of two *independent* series differ by 4.5 cm²/sec² given the expected deviation of an average to be 11 cm²/sec² is order 50% (using normal distribution). Thus it is not improbable that the averages of the first and last 300 days of the record should be within 4.5 cm²/sec² of each other.

Schmitz (1976b) has recently reported on estimates of mean velocities in many locations in the western North Atlantic. If we extrapolate the conclusions from the MODE spectra above to the other locations he discusses, then we would expect large uncertainties to be present in his estimates; this is qualitatively borne out by his Figures 2 and 5. Schmitz (1976c) describes a relatively strong mean current of 2.0 ± .3 cm/sec at 4000 m in the eastern part of the MODE region. If we were to assume, as a simplest alteration which allows us to use the previously calculated error values, that the velocity spectrum there were similar to Figure 9, except about 50% weaker (to give a variance ~ 10 cm²/sec²), then our estimate of the uncer-

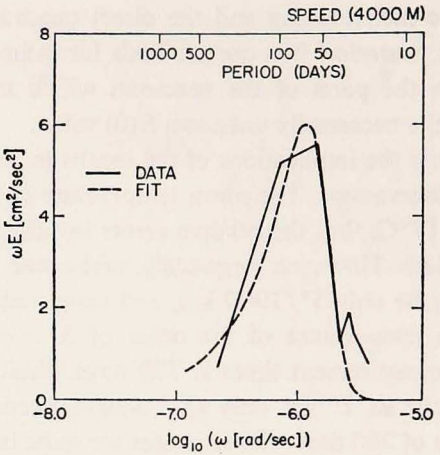

Figure 9. A kinetic energy spectrum from 4000 m depth near 28°N, 70°W (from Schmitz, personal communication) plus the optimal fit.

tainty at 700 d would be $\pm$ .4 from Table 2. As in the comparison of the variance estimate described above, the 700 d variance error estimates are similar here, but the small uncertainties for shorter times suggested by his Figure 2 are, in our opinion, fortuitous.

As a final application of our error formulae to current meter data, we estimated the errors in $\overline{u'v'}$ estimates from the same records as in Figures 8-9. The technique was direct numerical quadrature using the exact formula (2.15). Not surprisingly, these errors were comparable to, but larger than, those for the variance estimates: for $T = 700$ d, we estimate the relative uncertainties in $\overline{u'v'}$ at 500 and 4000 m, respectively, as 0.7 and 0.3.

d. Prospects for measuring mesoscale moments. Presented in § 4C was an application of the three parameter model to particular observations and an evaluation of the errors in present estimates of means and variances. We can extend this discussion somewhat and ask what is the measurement time required to achieve a certain level of accuracy in the more difficult of these measurements, the variance. From Table 1 we can estimate the r.m.s. relative error for very large times as

$$\sqrt{\epsilon_2}/\sigma^2 = \sqrt{C/T^*}$$

where C is a complicated function of η. The range of C is small, however: for $\eta = 0$, $C = 2.5$, and for $\eta \to \infty$, $C \to 1.9$. If we therefore choose a typical C as 2.2, then a relative error of one-tenth can only be achieved for $T_* \gtrsim 220$. From the ω_0 values in Table 2, we can estimate the required record lengths for ten percent variance accuracy as 15 years (T_{500}), 28 years (V_{500}), and 14 years (V_{4000}). If these numbers are typical of mid-latitude eddy processes, then one must admit that a

statistical documentation of them, encompassing their geographical diversity, is a formidable task. While ten or twenty years does not exceed the working career of a scientist—nor do the resources required exhaust present levels of public support for oceanography—one must nevertheless be certain there are not more informative quantities that could be measured with greater economy. On the other hand, measuring these statistics to discover gross qualitative features of the ocean environment is well worthwhile. An example of this is Schmitz's (1976a) demonstration of differences by a factor of 100 in the magnitude of eddy energy in the North Atlantic.

Acknowledgments. We appreciate the support of this research by the National Science Foundation through its grant to the National Center for Atmospheric Research. We are especially grateful to Dr. William Schmitz for sharing with us his unpublished spectra. This study is MODE Contribution No. 72.

APPENDIX

1. *Error in the estimate of the mean.*

From (2.3) and (2.1) we find

$$\bar{\phi} = \langle\phi\rangle + \int_{-\infty}^{\infty} d\omega\, \Phi(\omega) \frac{1}{T} \int_{-T/2}^{T/2} dt\, e^{-i\omega t}$$

$$= \langle\phi\rangle + \int_{-\infty}^{\infty} d\omega\, \Phi(\omega)\, S(\omega T/2) \ . \tag{A.1}$$

Substituting this into (2.4) gives

$$\epsilon_1 = \Big\langle \int_{-\infty}^{\infty} d\omega\, \Phi(\omega)\, S(\omega T/2) \int_{-\infty}^{\infty} d\omega'\, \Phi(\omega')\, S(\omega' T/2) \Big\rangle$$

$$= \int_{-\infty}^{\infty} d\omega \int_{-\infty}^{\infty} d\omega'\, S(\omega T/2)\, S(\omega' T/2)\, E(\omega)\, \delta(\omega+\omega') \ ,$$

which leads directly to (2.5).

2. *Asymptotic formulae.*

The formulae (2.13)-(2.15) may be derived by a direct application of the following two asymptotic relations:

$$\int_{-\infty}^{\infty} d\omega\, F(\omega)\, S^2(\omega T/2) \sim {}^{2\pi}/_{T}\, F(0) + {}^{1}/_{T^2} \int_{-\infty}^{\infty} d\omega\, \frac{F(\omega) + F(-\omega) - 2F(0)}{\omega^2}$$

$$+ o(1/T^N) \text{ as } T \to \infty \tag{A.2}$$

$$\int_{-\infty}^{\infty} d\omega \int_{-\infty}^{\infty} d\omega'\, A(\omega)\, B(\omega)\, S[(\omega-\omega')T/2]\, S(\omega T/2)\, S(\omega' T/2)$$

$$\sim \frac{4\pi^2}{T^2} A(0)\, B(0) + O({}^{1}/_{T^3}) \ . \tag{A.3}$$

To prove (A.2), let

$$I \equiv \int_{-\infty}^{\infty} d\omega\, F(\omega)\, S^2\left(\frac{\omega T}{2}\right) = \int_{-\infty}^{\infty} d\omega\, \hat{F}(\omega)\, S^2(\omega T/2)\ ,$$

where $\hat{F}(\omega) = \frac{1}{2}[F(\omega) + F(-\omega)]$ is an even function of ω. The integral I can also be written as

$$I = \hat{F}(0) \int_{-\infty}^{\infty} d\omega\, S^2(\omega T/2) + \frac{4}{T^2} \int_{-\infty}^{\infty} d\omega\, \hat{F}_1(\omega) \sin^2(\omega T/2)$$

where $\hat{F}_1(\omega) = [\hat{F}(\omega) - \hat{F}(0)]/\omega_2$ which is bounded as $\omega \longrightarrow 0$. The first term in I can be evaluated explicitly, and the second can be split into two components:

$$I = \frac{2\pi}{T}\hat{F}(0) + \frac{2}{T^2}\int_{-\infty}^{\infty} d\omega\, \hat{F}_1(\omega) - \frac{2}{T^2}\int_{-\infty}^{\infty} d\omega\, \hat{F}_1(\omega) \cos \omega T$$

Through successive integrations by parts, the last term in I can be shown to decay faster than any negative power of T (n.b., the evenness of $\hat{F}_1(\omega)$ implies that all odd derivatives of $\hat{F}_1(\omega)$ vanish at the origin). This completes the proof of (A.2); (A.3) may be proved in a similar manner.

REFERENCES

Bendat, J. S., and A. G. Piersol. 1966. Measurement and Analysis of Random Data, New York, J. Wiley & Sons, 390 pp.

Frankignoul, C. 1976. Observed interactions between oceanic internal waves and mesoscale eddies, Deep-Sea Res., in press.

Jenkins, G. M. and D. G. Watts. 1968. Spectral Analysis and its Applications, San Francisco, Holden-Day, 525 pp.

Lumley, J., and H. Panofsky. 1964. The Structure of Atmospheric Turbulence, New York, J. Wiley & Sons, 239 pp.

Müller, P. 1974. On the interaction between short internal waves and larger scale motions in the ocean, Hamburg Geophys. Einzelshriften, *23*.

Schmitz, W. J. 1976a. Eddy kinetic energy in the deep western North Atlantic, J. Geophys. Res., Oceans and Atmospheres, *81*, 4981–4982.

—— 1976b. On the deep general circulation in the western North Atlantic, J. Mar. Res., *35*, 21–28.

—— 1976c. Observation of a new abyssal current at the western front of the Bermuda Rise, Geophys. Res. Ltrs., *3*, 373–374.

Webster, F. 1969. Turbulence spectra in the ocean, Deep-Sea Res., *16*, supp., 356–358.

Wunsch, C. 1972. The spectrum of temperature near Bermuda from two minutes to two years, Deep-Sea Res., *19*, 577–593.